Published in final edited form as:

Biochim Biophys Acta Mol Cell Biol Lipids. 2017 March ; 1862(3): 324–336. doi:10.1016/j.bbalip.2016.12.004.

Deficiency of glycerol-3-phosphate acyltransferase 1 decreases triacylglycerol storage and induces fatty acid oxidation in insect fat body

Michele Alves-Bezerra[a,b], **Isabela B. Ramos**[a], **Iron F. De Paula**[a], **Clarissa M. Maya-Monteiro**[c], **Eric L. Klett**[b,d], **Rosalind A. Coleman**[b], **Katia C. Gondim**[a,*]

[a]Instituto de Bioquímica Médica Leopoldo de Meis, Universidade Federal do Rio de Janeiro, Rio de Janeiro, RJ, Brazil

[b]Department of Nutrition, University of North Carolina, Chapel Hill, NC 27599, USA

[c]Instituto Oswaldo Cruz, Fundação Oswaldo Cruz, Rio de Janeiro, RJ, Brazil

[d]Department of Medicine, University of North Carolina, Chapel Hill, NC 27599, USA

Abstract

Glycerol-3-phosphate acyltransferases (GPAT) catalyze the initial and rate-limiting step for the *de novo* synthesis of triacylglycerol (TAG). Four mammalian GPAT isoforms have been identified: the mitochondria-associated GPAT1 and 2, and the endoplasmic reticulum(ER)-associated GPAT3 and 4. In the insect *Rhodnius prolixus*, a vector of Chagas' disease, we previously predicted a mitochondrial-like isoform (RhoprGPAT1) from genomic data. In the current study, we clone the RhoprGPAT1 coding sequence and identify an ER-associated GPAT (RhoprGPAT4) as the second isoform in the insect. RhoprGPAT1 contributes 15% of the total GPAT activity in anterior midgut, 50% in posterior midgut and fat body, and 70% in the ovary. The *RhoprGpat1* gene is the predominant transcript in the midgut and fat body. To evaluate the physiological relevance of RhoprGPAT1, we generate RhoprGPAT1-deficient insects. The knockdown of *RhoprGpat1* results in 50% and 65% decrease in TAG content in the posterior midgut and fat body, respectively. *RhoprGpat1*-deficient insects also exhibits impaired lipid droplet expansion and a 2-fold increase in fatty acid β-oxidation rates in the fat body. We propose that the RhoprGPAT1 mitochondrial-like isoform is required to channel fatty acyl chains towards TAG synthesis and away from β-oxidation. Such a process is crucial for the insect lipid homeostasis.

Keywords

Beta-oxidation; Fatty acid metabolism; Lipids; Triacylglycerol synthesis; Fatty acid oxidation; Insect physiology

*Corresponding author at: Av. Carlos Chagas Filho, 373, Cidade Universitária, Rio de Janeiro, RJ, Brazil., katia@bioqmed.ufrj.br (K.C. Gondim).

Supplementary data to this article can be found online at http://dx.doi.org/10.1016/j.bbalip.2016.12.004.

Transparency Document

The Transparency document associated with this article can be found, in online version.

1. Introduction

The synthesis of triacylglycerol (TAG) is initiated by the acylation of glycerol-3-phosphate (G3P) with a long-chain acyl-CoA in a rate-limiting step catalyzed by glycerol-3-phosphate acyltransferase (GPAT). Four GPAT isoforms have been identified in mammals: GPAT1 and 2 are mitochondria-associated proteins, whereas GPAT3 and 4 are located on the endoplasmic reticulum (ER). The contribution of each isoform to lipid metabolism varies in a tissue- and nutritionally-dependent manner. GPAT1 activity constitutes about 10% of total GPAT activity in most of tissues except for liver, where it corresponds to 30–50% of the total activity [1]. *Gpat1*$^{-/-}$ mice have reduced body weight, lower hepatic TAG content and increased hepatic β-oxidation [2]. When fed a high-fat diet, *Gpat1*$^{-/-}$ mice resist hepatic steatosis and maintain enhanced insulin sensitivity [3]. The abundance of *Gpat2* mRNA is 50-fold greater in testis than in lipogenic tissues [4]; in testis GPAT2 acts to incorporate arachidonoyl-CoA (20:4) into TAG, thereby regulating the availability of polyunsaturated acyl-chains within spermatogenic cells [5]. GPAT3 contributes nearly 80% of total GPAT activity in murine white adipose tissue [6]. GPAT3-deficient animals have reduced fat mass and increased hepatic TAG and cholesteryl ester content [7]. GPAT4 contributes 40–50% of total hepatic GPAT activity and is required for the incorporation of exogenous fatty acids into TAG [2]. GPAT4 is also the major GPAT isoform in brown adipose tissue (BAT), where it is important in the partitioning of exogenous acyl-CoAs into lipid droplet TAG and away from mitochondrial β-oxidation [8].

Information about GPAT enzymes is scarce among non-mammalian animals, such as arthropods. GPAT activity was detected in the Mediterranean fruit fly *Ceratitis capitata* [9] and inferred in the tobacco hornworm *Manduca sexta* based on lipid synthesis measurements [10]. In the silkworm *Bombyx mori*, the knockdown of a putative GPAT protein results in decreased TAG content in pheromone glands [11]. A mitochondrial GPAT activity was characterized in the shrimp *Macrobrachium borelii* [12], but the presence of multiple isoforms remains unknown. The overexpression of *Drosophila melanogaster* mitochondrial-like GPAT increases lipid accumulation in larvae salivary glands [13]. Additionally, two microsomal-like isoforms (dmGPAT3 and 4) were identified in the fruit fly [14], and the migration of dmGPAT4 from ER to lipid droplets (LDs) is required for LD expansion [15].

In *Rhodnius prolixus*, a hematophagous insect and vector of Chagas' disease in Central and South America, lipids are required not only for basic cellular functions, but also for survival during prolonged starvation and for reproduction [16,17].

A mitochondrial-like GPAT (*RhoprGpat1*) gene, predicted from genomic data, was suggested to initiate the glycerolipid synthesis in the gut and in the fat body – an organ functionally analogous to both mammalian liver and adipose tissue – after a blood meal [18]. Here we show that an additional microsomal-like GPAT (RhoprGPAT4) is also present in this insect. Because RhoprGPAT1 comprised about 50% of total GPAT activity in the posterior midgut and fat body, was the predominant transcript in both organs, and was up-regulated after feeding, we hypothesized that RhoprGPAT1 must play a critical role in TAG synthesis in fed animals. To test this hypothesis, we evaluated lipid metabolism in

insects after knocking down RhoprGPAT1. Our studies show that the lack of RhoprGPAT1 prevented fatty acid incorporation into TAG and increased fatty acid β-oxidation.

2. Material and methods

2.1. Insects

Insects were taken from a colony of *Rhodnius prolixus* maintained at 28 °C and 70–75% relative humidity, and were fed with live-rabbit blood at 3-week intervals [17]. All animal care and experimental protocols were conducted following the guidelines of the Committee for Evaluation of Animal Use for Research from the Federal University of Rio de Janeiro (CAUAP-UFRJ) and the NIH Guide for the Care and Use of Laboratory Animals (ISBN 0–309-05377–3). The protocols were approved by CAUAP-UFRJ. Technicians dedicated to the animal facility at the Institute of Medical Biochemistry (UFRJ) conducted all aspects related to rabbit husbandry under strict guidelines to ensure careful and consistent animal handling.

2.2. Gene identification

Genes were searched in the *R. prolixus* genome assembly (VectorBase, http://www.vectorbase.org, *R. prolixus* CDC annotation, RproC1) by similarity to the acyltransferase family consensus sequence (Pfam number PF01553) using FAT software [19]. Identified supercontigs were compared by tBlastn to GPAT protein sequences from different organisms available in GenBank. Coding region prediction, protein primary sequence and phylogenetic analyses were performed as described [17]. Subcellular localization was predicted by PSORT II Server [20].

2.3. Rapid amplification of cDNA 5′-end (5′-RACE)

The 5′ end of the *RhoprGpat1* was amplified using GeneRacer kit for full-length, RNA ligase-mediated rapid amplification of 5′ and 3′ cDNA ends (RLM-RACE, Invitrogen). Amplification of the full-length cDNA was performed using primers designed for specific amplification of target genes based on *in silico* predictions and the information obtained using RACE (Supplementary Table 1). PCR reactions were carried out as described [21]. The full length CDS sequences obtained for *RhoprGpat1* or *RhoprGpat4* were registered in the NCBI GenBank database under accession numbers KT328599 and KT328600, respectively.

2.4. Quantitative PCR (qPCR)

Organs were obtained as described [18], and total RNA was isolated from samples (pools from 3 to 5 organs), treated with RNase-free DNase I and used to synthesize cDNA. qPCR was performed using specific primers for the target genes (Supplementary Table 1) [21]. *Rhopr18S* gene amplification was used for normalization [22]. Primer efficiencies and qPCR inhibition were determined [23]. Amplification specificity analysis and qPCR controls to detect contaminations were conducted following the MIQE guidelines [24].

2.5. GPAT assay

Organs (obtained from 16 to 25 insects) were homogenized in a Potter-Elvehjem tube (30 strokes) in cold Medium I buffer (250 mM sucrose, 10 mM Tris, pH 7.4, 1 mM EDTA, 1 mM dithiothreitol). Samples were centrifuged at 3000 g for 15 min at 4 °C, and total membranes were isolated from the supernatant by centrifuging at 150,000 g for 1 h at 4 °C. *sn*-[2-^{3}H]glycerol 3-phosphate was synthesized enzymatically [25]. Efficiency of synthesis reaction was checked by paper chromatography, and obtained [3H]glycerol 3-phosphate was purified by anion exchange chromatography, as described [25]. GPAT activity was assayed for 10 min at room temperature in a 200 μL mixture containing 3 μCi [3H]glycerol 3-phosphate (specific activity 19 mCi/mmol), supplemented with 800 μM glycerol 3-phosphate, 80 μM palmitoyl-CoA, 75 mM Tris-HCl, pH 7.5, 4 mM $MgCl_2$, 1 mg/mL fatty acid-free albumin, 1 mM DTT, and 8 mM NaF [26]. After incubating samples on ice for 15 min in the presence or absence of 2 mM *N*-ethylmaleimide (NEM), the reaction was initiated by adding 4–8 μg of membrane protein to the assay mixture. The reaction products were extracted into $CHCl_3$ and 1% perchloric acid as described [27], and the radioactivity present in the organic phase, was determined by scintillation counting. >98% of the products extracted in this way were lysophosphatidic acid and also phosphatidic acid, rapidly synthesized from the former. NEM-resistant activity (RhoprGPAT1) was calculated by subtracting NEM-sensitive activity (RhoprGPAT4) from total activity.

2.6. Gene knockdown and insect treatment

dsRNA was synthesized by MEGAScript RNAi Kit (Ambion Inc., Austin, USA) using primers for *RhoprGpat1* specific gene amplification (Supplementary Table 1) [17]. RNAi specificity was confirmed by off-target search using dsCheck software [28]. Unfed adult females were injected with 0.5 μg dsRNA [17] and fed 3 days later. Knockdown efficiency was confirmed in each experiment by qPCR, and knockdown persistence was also determined (Suppl. Fig. 1). The bacterial *MalE* gene was used as a control dsRNA [29].

2.7. Phenotypic analyses

Adult females injected with dsRNA were fed with live-rabbit blood and immediately transferred to individual vials. The mortality rates and the number of laid eggs were recorded daily. Protein digestion analysis, enzymatic TAG determination, *de novo* lipid synthesis assay, and fatty acid oxidation assay were performed as described [21]. Briefly, for fatty acid oxidation assay, ten days after blood meal the insects were dissected and five fat bodies were obtained from each experimental group. Organs were washed in 0.15 M NaCl and homogenized in a Potter-Elvehjem tube (15 strokes) in 200 μL of cold buffer H (10 mM Hepes-KOH, pH 7.4, 0.25 M sucrose, 1 mM EDTA, 1 mM DTT) containing 0.002% v/v protease inhibitor cocktail (Sigma-Aldrich Co., St. Louis, USA). The homogenate (150 μg protein) was incubated with 8 μCi ^{3}H-palmitate (0.1 μCi/μL; Perkin-Elmer) in 75 mM Tris–HCl, pH 7.4, 2 mM $MgCl_2$, 2 mg/mL fatty acid free albumin, 5 mM ATP, 5 mM DTT, 0.2 mM CoASH, 10 mM L-carnitine, 20 mM palmitate (200 μL final volume) at 28 °C for 30 min. Reactions were stopped with 200 μL cold perchloric acid (24%) and incubated at 4 °C overnight to precipitate palmitate-bound albumin. Supernatants (300 μL) were centrifuged at

14,000 rpm and 4 °C for 5 min and lipids were extracted into $CHCl_3$ [30]. Radioactivity of the oxidized products in the aqueous phase was measured using a liquid scintillation counter.

2.8. Lipid analysis

Three days after dsRNA injection, adult females were fed with rabbit blood supplemented with ^{32}Pi (0.1 μCi/μL of blood; IPEN/CNEM, São Paulo, Brazil) and 10 mM EDTA. Lipophorin was purified from hemolymph collected on the 4th day after feeding and its density was determined as described [31]. For lipid composition analysis, hemolymph was collected from dsRNA-injected insects, also on the 4th day after feeding. Samples were centrifuged at 13,000 *g* for 5 min to remove cells, and lipids were extracted from the supernatant as described [30]. Anterior and posterior midguts were dissected on the 2nd day, when the midgut shows high rates of lipid synthesis and transfer to lipophorin [32]. The laid eggs were obtained on the 5th day after feeding, from females which were also dissected for fat body separation. This day was chosen because females have just started to lay eggs, and the fat body shows increased *RhoprGpat1* mRNA levels [18]. Organs were washed in cold 0.15 M NaCl, homogenized with a Potter-Elvehjem tube (25 strokes) in 250 μL of the same solution, and lipids were extracted. Neutral lipid or phospholipids (PL) were separated by TLC [33,34]. The plates were stained with copper reagent [35] and the lipid composition was determined by densitometric analysis using the software TotalLab Quant v11 (TotalLab Ltd., Newcastle, United Kingdom).

2.9. Nile Red staining of the lipid droplets

Fat bodies were obtained from dsRNA injected insects on the 10th day after feeding (at least three females from each condition), and stained with Nile Red, as previously described for *R. prolixus* lipid droplets analysis [36]. The fat bodies were incubated for 15 min in 0.001% Nile Red (Sigma-Aldrich) and 40 μg/mL DAPI (Sigma-Aldrich) made up in 75% glycerol. Tissues were mounted in 100% glycerol and immediately imaged in a Leica TCS-SPE laser scanning confocal microscope, in two independent experiments. The excitation wavelengths used were 543 nm for Nile Red and 280 nm for DAPI. Z-stacks were obtained from 20 to 25 optical sections (1.5 μm each) using a 20× objective, and the peripheral regions of the fat bodies were analyzed. The average diameters of the lipid droplets were obtained from a representative image of each insect group, using the DAIME image analysis software after edge detection automatic segmentation [37].

2.10. Statistical analyses

$\Delta\Delta C_t$ mean values obtained from qPCR experiments were submitted to Grubb's test to detect outliers [38], and the comparison among different conditions was made using One-way ANOVA followed by Tukey's multiple comparison test. Differences were considered significant at $P < 0.05$. The relative expression values ($2^{-\Delta\Delta Ct}$) were used only for graph construction.

Differences in survival curves were analyzed using the Log-Rank test and considered significant at $P < 0.05$. Other results were analyzed by Student's *t*-test for the comparison of two different conditions, One-way ANOVA followed by Tukey's test or Two-way ANOVA followed by Bonferroni correction for the comparison among more than two conditions.

Differences were considered significant at $P < 0.05$. All statistical analyses were performed using the Prism 5.0 software (GraphPad Software, San Diego, USA).

3. Results

3.1. Gene identification and sequence analyses

Based on the initial sequence predicted for a *R. prolixus* mitochondrial-like GPAT [18], we cloned the full-length coding sequence of this gene. The obtained sequence (NCBI accession number KT328599), renamed as RhoprGPAT1, differs from a previous report [18] at the 3′-end (data not shown) and encodes an 818-amino acid protein (Fig. 1A). A second GPAT isoform, RhoprGPAT4 (NCBI accession number KT328600), was also cloned (Fig. 1). Both proteins contain the four conserved motifs (I–IV) found in the GPAT enzymes (Fig. 1A and Table 1) [39]. Phylogenetic analysis showed that RhoprGPAT1 is similar to the mitochondrial GPAT isoforms, whereas RhoprGPAT4 clustered with microsomal isoforms (Fig. 1B). Although we were unable to identify additional GPAT-encoding genes in *R. prolixus* genome, it remains unclear whether other GPAT isoforms could be generated by alternative mRNA processing. Alternatively, additional GPAT activity could be a result of unanticipated enzymatic function of other acyltransferase family members.

3.2. RhoprGpat1 and 4 genes were differentially regulated

Mammalian GPAT isoforms exhibit tissue-specific transcriptional patterns and are affected by nutritional status [1]. In *R. prolixus*, fatty acids derived from dietary lipids are absorbed by the enterocytes and used for the synthesis of complex lipids, including DAG and TAG [18, 42]. In the second day after feeding, intestinal biosynthetic activity reaches its maximal activity and the newly synthesized lipids are transported via hemolymph to other tissues by lipophorin [32,42,43]. The fat body stores lipids mainly as TAG [18], with a maximal TAG storage capacity being reached around the 5th day after feeding [16]. *RhoprGpat1* transcription was previously shown to be up-regulated in the anterior midgut and posterior midgut after the blood meal [18]. To determine whether *RhoprGpat4* is similarly regulated, mRNA abundance was determined in different organs under varying physiological conditions. Transcripts were measured in the anterior midgut (stomach), posterior midgut (intestine) and fat body at different days after feeding, including initial and later stages of digestion and lipid accumulation. On the 4th day after a blood meal, when most of organs are highly metabolically active, the *RhoprGpat4* transcript was less abundant than that of *RhoprGpat1* in the posterior midgut and in the fat body (Fig. 2A). However, the mRNA levels were similar for both genes in the anterior midgut and ovary (Fig. 2A). In contrast to the *RhoprGpat1* gene [18], RhoprGpat4 transcription varied neither in tissues after feeding (Fig. 2B–D) nor during follicle grow and maturation (Fig. 2E), in spite of a trend of increased *RhoprGpat4* transcription observed in the anterior midgut on the day 10 after feeding (Fig. 2B, $P = 0.09$ when compared to unfed insects).

3.3. RhoprGPAT1 and 4 activities exhibited tissue-specific variation

To compare the contributions of RhoprGPAT1 and RhoprGPAT4 to total GPAT activity, we measured GPAT specific activity in the presence and absence of NEM (*N*-ethylmaleimide). NEM inhibits the mammalian GPAT2, 3 and 4 isoforms, but neither mammalian GPAT1 [1]

nor arthropod mitochondrial GPAT activity [12] is affected. On the 4th day after feeding, when the analyzed organs are metabolically very active, the NEM-resistant RhoprGPAT1 activity contributed 15% of the total GPAT activity in anterior midgut, approximately 50% in posterior midgut and fat body, and 70% in the ovary (Fig. 3).

3.4. RhoprGpat1-deficient insects retained NEM-sensitive GPAT activity

Because *RhoprGpat1* exhibited a nutritionally-regulated expression pattern [18] and contributed substantially to total GPAT activity in the posterior midgut and fat body, which are highly committed to lipid biosynthesis (Fig. 3), we predicted that this enzyme would have a major role in the TAG metabolism. To test this hypothesis, we performed a dsRNA-mediated knockdown of *RhoprGpat1*. When compared to control insects, total GPAT specific activity in the midgut of *RhoprGpat1*-deficient animals on the 2nd day after feeding was 30% lower, NEM-resistant GPAT activity was reduced by 85%, but NEM-sensitive GPAT activity remained nearly unchanged (Fig. 4A). In the fat body of knocked down insects on the 5th day after feeding, total GPAT specific activity was 60% lower, residual NEM-resistant GPAT activity was present (<10%), and the NEM-sensitive activity was reduced by 40% (Fig. 4B). These time points were chosen for this comparison as *RhoprGpat1* expression is highest at these days in each organ, as previously described [18].

3.5. RhoprGpat1 knockdown affects the expression of lipid-related genes

To determine whether *RhoprGpat4* isoform was affected by the absence of RhoprGPAT1, we measured its mRNA expression after gene silencing. In the anterior midgut and ovary of *RhoprGpat1*-deficient animals, the transcript abundance of *RhoprGpat4* was 20% higher than in control insects (Fig. 5A and D). Significant variations in *RhoprGpat4* mRNA levels were not detected in the posterior midgut and fat body (Fig. 5B and C).

Fatty acids, acyl-CoAs, and their derivatives are endogenous ligands for several transcription factors that control cellular energy metabolism [44–46]. Because reduced GPAT activity affects the intracellular content of lipid intermediates, we hypothesized that the *RhoprGpat1* knockdown would affect the transcription of genes related to lipid metabolism. Compared to control animals, in the anterior midgut of *RhoprGpat1*-silenced animals on the 2nd day after feeding, transcription of the long-chain acyl-CoA synthetase 1 (*RhoprAcsl1*) gene was 50% higher (Fig. 5A). In the posterior midgut, the acyl-CoA-binding protein 1 (*RhoprAcbp1*) mRNA abundance was 40% lower (Fig. 5B). The carnitine palmitoyltransferase 1 (*RhoprCpt1*) gene was affected both in fat body and ovary (2.3-fold increase and 20% decrease, respectively) on the 5th day after feeding (Fig. 5C–D).

3.6. In the absence of RhoprGPAT1, longevity, circulating lipids and oviposition were not affected

To ascertain the impact of *RhoprGpat1* knockdown on some physiological parameters of the kissing bug, we measured the lifespan during a 6-week starvation and the digestive rate of dsRNA treated animals. Compared to controls, RhoprGPAT1-deficient animals did not exhibit any significant changes (Fig. 6A and B).

Because lipophorin is a major lipoprotein present in the hemolymph of insects [47], we determined whether its lipid loading would be affected. On the 4th day after feeding the absence of RhoprGPAT1 changed neither lipophorin density (1.131 ± 0.004 and 1.135 ± 0.001 g/mL in control and knocked down insects, respectively) nor hemolymphatic lipid composition (Fig. 6C and D). Moreover, RhoprGPAT1-deficiency affected neither oviposition nor the rate of viable nymphs hatching from eggs (Fig. 6E and F).

3.7. RhoprGPAT1-deficiency reduces TAG content

The monthly blood meal drives enterocyte lipogenesis in *R. prolixus*, in the early days after feeding, as well as fat body TAG storage and ovarian follicle maturation during subsequent days [16,18,42,48]. Because our data suggested that RhoprGPAT1 contributes substantially to lipid synthesis (Fig. 3), we asked whether the knockdown of this protein would alter the lipid composition of insect organs. In anterior midgut compared to control animals, phosphatidic acid (PA) content was reduced by 30% (Fig. 7A). Posterior midgut and fat body exhibited 50% and 65% reductions in TAG content, respectively (Fig. 7B and C). Eggs laid by knocked down females had a 15% reduction in TAG content (Fig. 7D).

In insects, the fat body is the main organ for lipid storage [49]. To understand how the TAG content of the fat body changes over time, we measured TAG on different days after feeding. We found that RhoprGPAT1-deficient fat bodies contained less TAG from day 7 to day 10 after feeding (Fig. 8A), although the protein content was not affected (Fig. 8B). Drosophila S2 cells contain two populations of TAG-containing LDs, smaller LDs and large, expanding LDs. Since the density of the large LDs increases under lipogenic stimuli [15,50], we examined the average size of Nile Red stained LDs to determine whether the knockdown of *RhoprGpat1* affected LD expansion. Compared to unfed animals, fat bodies from fed control animals had a higher density of large LDs whose average diameter was 7.0 ± 4.8 μm (Fig. 8C and D, Suppl. Fig. 2). In contrast, on the 10th day after feeding, RhoprGPAT1-deficient fat bodies had a prevalence of smaller LDs whose average diameter was 4.0 ± 2.0 μm (Fig. 8C and D, Suppl. Movies 1 and 2).

3.8. RhoprGpat1 knockdown reduced the incorporation of de novo synthesized fatty acid into lipids and increased fatty acid oxidation

GPAT1 is linked to *de novo* lipogenesis in mice hepatocytes by the incorporation of newly synthesized fatty acids into TAG and PL [2]. Using [^{3}H]acetate, we measured the ability of *RhoprGpat1* knocked down insects to synthesize fatty acids *de novo* and incorporate them into glycerolipids. In the fat body of RhoprGPAT1-deficient animals, the amount of [^{3}H]acetate incorporated into lipids was 30% lower than in controls (Fig. 9A).

Previous studies have suggested that GPAT1 competes with CPT1 for acyl-CoA at the outer mitochondrial membrane [2,51,52]. To examine this effect in the kissing bug, we measured the oxidation of [^{3}H]palmitate by the fat body. Compared to control animals, the knockdown of *RhoprGpat1* resulted in a 2-fold increase in fatty acid oxidation (Fig. 9B).

4. Discussion

GPAT isoenzymes catalyze the rate-limiting step in the synthesis of TAG and are important regulators of lipid homeostasis. Based on their subcellular localization, these proteins are classified into two distinct groups: the mitochondria- and the microsome-associated GPATs. In *R. prolixus*, we found two isoforms of GPAT (RhoprGPAT1 and RhoprGPAT4), encoded by independent genes (Fig. 1A and Table 1) [18]. Although the presence of another GPAT gene in *R. prolixus* cannot be totally discarded, only two genes were found in the insect genome [53]. Part of the primary sequence of RhoprGPAT1 was previously described and a phylogenetic analysis revealed that it is closely related to the mammalian mitochondrial GPAT isoforms [18]. RhoprGPAT4 was grouped among the microsomal isoforms (Fig. 1B and Table 1). All the other Arthropoda species analyzed also had two GPAT isoforms and exhibited the same phylogenetic pattern that was observed in *R. prolixus* (Fig. 1B). The single exception was *D. melanogaster*, for which one mitochondrial-like isoform (DromeGPAT1) and two microsomal-like isoforms (DromeGPAT3 and 4) were reported [14].

Because *S. cerevisiae* does not follow this pattern, our data suggest that the divergence between mitochondrial and microsomal GPATs occurred in the Animalia phylum (Fig. 1B). Moreover, the presence of two mitochondrial and two microsomal isoforms could be a result of gene duplication events that occurred after the emergence of chordates (Fig. 1B). The presence of distinct GPAT isoforms suggests a gain of specialized functions, and this hypothesis is strongly supported. For example, the absence of GPAT1, but not GPAT4, results in reduced incorporation of *de novo* synthesized fatty acids into TAG and increased β-oxidation in the liver [2]. In 3T3-L1 adipocytes, the knockdown of GPAT3, which is induced during differentiation, reduces lipid accumulation and downregulates the expression of adipogenic markers (PPARγ and SREBP1c). However, a knockdown of the second microsomal isoform, GPAT4, results in a different phenotype [54].

In *R. prolixus, RhoprGpat1* is modulated transcriptionally in lipogenic organs [18]. After a blood meal, the dietary lipids are hydrolyzed in the midgut lumen and released fatty acids are absorbed by the enterocytes. In these cells, the lipid substrates are channeled for the synthesis of a variety of glycerolipids via the G3P pathway [18,42] and the biosynthetic activity seems to be maximal until the second day after feeding [32]. Newly synthesized lipids are transferred to lipophorin and transported to other tissues, primarily as DAG [32,42,43]. In the fat body, lipids derived from lipophorin are directed into TAG synthesis [18], and the maximal TAG level in this organ is observed around the 5th day after feeding [16]. Since *RhoprGpat1* transcription in the midgut increases during the first and second days after feeding [18], concomitant with the use of dietary fatty acids for lipogenesis [42], and induced later in the fat body [18] at a time of maximal TAG accumulation by the insect [16], it was suggested that RhoprGPAT1 is important for *R. prolixus* lipogenesis [18].

Although *RhoprGpat1* transcripts showed highest abundance (Fig. 2A), the NEM-sensitive GPAT specific activity, which probably reflects RhoprGPAT4 activity (Fig. 4), contributed 85% of total GPAT activity in the anterior midgut and nearly 50% in the posterior midgut and fat body (Fig. 3). A similar discrepancy between mRNA levels and enzymatic activity

was previously reported for mammalian GPAT isoforms [55], and post-transcriptional control mechanisms for GPAT activity have been described. Rodent GPAT1 is potentially activated by phosphorylation by casein kinase 2 [56], whereas AMPK inhibits GPAT1 activity and reduces lipogenesis in rat liver and skeletal muscle [57]. The microsomal GPAT activity of rat adipose tissue was reported to be inhibited by treatment with PKA and reactivated by alkaline phosphatase [58]. In *D. melanogaster*, the intracellular dynamics of DromeGPAT4 limits its contribution to TAG synthesis. Upon lipogenic stimulus, this protein relocalizes from the E.R. to LDs and is believed to be required for LDs expansion [15].

The intermediate products in the pathway of TAG synthesis are intracellular signals. GPAT1 overexpression in mouse hepatocytes increases the intracellular content of lysophosphatidic acid (LPA), PA and DAG, and leads to reduced insulin-stimulated Akt phosphorylation as well as inhibition of mTORC2 [59]. Moreover, GPAT4-deficient mice have improved insulin responsiveness because of enhanced association of mTOR/rictor and an increase in mTORC2 activity [60].

LPA is a ligand for peroxisome proliferator-activated receptor (PPAR) γ [61]. Increased LPA content in GPAT1-overexpressing CHO cells results in PPARγ activation, suggesting a role for LPA in regulating gene expression [44]. In *R. prolixus*, *RhoprGpat1* disruption resulted in altered expression of *Acsl1*, *Acbp1*, and *Cpt1* (Fig. 5). Although the mechanism underlying this effect remains unclear, it is possible that changes in lipid intermediates in insects affects the activity of transcriptional factors that regulate lipid-related genes. The physiological function of RhoprACSL1 remains unknown, however a second ACSL isoform, RhoprACSL2, is required for the activation of a long chain fatty acid pool directed to β-oxidation in the fat body of *R. prolixus* [21]. The acyl-CoA-binding protein RhoprACBP1 contributes to the incorporation of fatty acid chain into TAG in the fat body [62]. Together with RhoprCPT1, likely to act as a regulator of fatty acid oxidation, the transcriptional modulation of these genes may affect the lipid homeostasis in the insect.

GPAT1 and its orthologues among different species have emerged as the main contributors for the production of the LPA pool used in TAG synthesis in liver and also in analogous organs, such as the crustacean hepatopancreas. In mice, GPAT1-deficiency reduces hepatic and plasma TAG levels and decreases VLDL secretion [51]. Conversely, GPAT1 overexpression increases the intracellular content of TAG [63,64]. In the shrimp *M. borellii*, a GPAT1-like isoform was identified in the hepatopancreas and was correlated with lipid synthesis in this organ [12]. The knockdown of *RhoprGpat1* in *R. prolixus* resulted in 65% decrease in TAG content in the fat body, 30% in posterior midgut, and 15% in eggs (Fig. 7). Additionally, RhoprGPAT1 deficiency impaired the ability of insects to accumulate TAG stores after feeding (Fig. 8A). Defective TAG accumulation was also evident in fluorescent microscopy experiments, in which the average diameter of LDs in the fat body of fed animals was greatly diminished in the absence of RhoprGPAT1 (Fig. 8C and D). Both the TAG content and the average LDs diameter of fed *RhoprGpat1*-deficient insects are comparable to those found in unfed animals (Fig. 8A, C, and D, Suppl. Fig. 2). Thus, RhoprGPAT1 is required in the fat body for *de novo* glycerolipid synthesis triggered by feeding.

GPAT1 localizes to the outer mitochondrial membrane where it can compete directly with CPT1 for long-chain acyl-CoA substrates. Therefore, GPAT1 might channel fatty-acid derivatives preferentially toward glycerolipid synthesis, counteracting their partitioning into the β-oxidation pathway [51,64]. In agreement with this hypothesis, GPAT1-deficient mice show reduced TAG content and increased fatty acid oxidation [2,3], and GPAT1 overexpression in rat hepatocytes doubles exogenous incorporation of fatty acids into TAG and causes a 40% decrease in β-oxidation [63]. Overexpression of GPAT1 also results in 10-fold increase in liver TAG and DAG content and a 25% decrease in lipid oxidation [65]. It is noteworthy that similar results were not found in GPAT4$^{-/-}$ mice [2], suggesting that the location of GPAT isoforms is a determinant for their roles in partitioning substrates between TAG synthesis and mitochondrial β-oxidation. In the fat body of *R. prolixus*, the knockdown of *RhoprGpat1* resulted in 30% decrease in *de novo* lipid synthesis and 2-fold increase in fatty acid oxidation (Fig. 9).

Our data demonstrate that the mitochondrial-like RhoprGPAT1 isoform regulates lipid metabolism in the fat body of *R. prolixus* after feeding by controlling fatty acid partitioning towards TAG synthesis and away from oxidation. As a novel finding among invertebrate species, this work provides key insights to understand the evolution and functions of GPAT enzymes in animals.

Supplementary Material

Refer to Web version on PubMed Central for supplementary material.

Acknowledgments

The authors thank Jorge M. Medina, Lilian S. C. Gomes and Heloisa S. L. Coelho for excellent technical assistance, and José de S. Lima Junior and Gustavo Ali for insect care. This work was supported by grants from Conselho Nacional de Desenvolvimento Científico e Tecnológico (CNPq) Grant 308119/2013-4, Coordenação de Aperfeiçoamento de Pessoal de Nível Superior (CAPES), Fundação de Amparo à Pesquisa do Estado do Rio de Janeiro (FAPERJ) Grant 201.591/2014, and Instituto Nacional de Ciência e Tecnologia em Entomologia Molecular (INCT-EM) Grant 573959/2008-0 (to K.C.G.), and U.S. National Institutes of Health (NIH) Grants DK56598 (to R.A.C.) and K08DK090141 (to E.L.K.).

Abbreviations:

ACBP1	acyl-CoA-binding protein 1
ACSL1	acyl-CoA synthetase 1
BAT	brown adipose tissue
CPT1	carnitine palmitoyltransferase 1
DAG	diacylglycerol
ER	endoplasmic reticulum
G3P	glycerol-3-phosphate
GPAT	glycerol-3-phosphate acyltransferase

LD	lipid droplet
LPA	lysophosphatidic acid
NEM	*N*-ethylmaleimide
PA	phosphatidic acid
PL	phospholipid
TAG	triacylglycerol

References

[1]. Coleman RA, Mashek DG, Mammalian triacylglycerol metabolism: synthesis, lipolysis, and signaling, Chem. Rev 111 (2011) 6359–6386. [PubMed: 21627334]

[2]. Wendel AA, Cooper DE, Ilkayeva OR, Muoio DM, Coleman RA, Glycerol-3-phosphate acyltransferase (GPAT)-1, but not GPAT4, incorporates newly synthesized fatty acids into triacylglycerol and diminishes fatty acid oxidation, J. Biol. Chem 288 (2013) 27299–27306. [PubMed: 23908354]

[3]. Neschen S, Morino K, Hammond LE, Zhang DY, Liu ZX, Romanelli AJ, Cline GW, Pongratz RL, Zhang XM, Choi CS, Coleman RA, Shulman GI, Prevention of hepatic steatosis and hepatic insulin resistance in mitochondrial acyl-CoA: glycerol-sn-3-phosphate acyltransferase 1 knockout mice, Cell Metab. 2 (2005) 55–65. [PubMed: 16054099]

[4]. Wang S, Lee DP, Gong N, Schwerbrock NMJ, Mashek DG, Gonzalez-Baro MR, Stapleton C, Li LO, Lewin TM, Coleman RA, Cloning and functional characterization of a novel mitochondrial N-ethylmaleimide-sensitive glycerol-3-phosphate acyltransferase (GPAT2), Arch. Biochem. Biophys 465 (2007) 347–358. [PubMed: 17689486]

[5]. Cattaneo ER, Pellon-Maison M, Rabassa ME, Lacunza E, Coleman RA, Gonzalez-Baro MR, Glycerol-3-phosphate acyltransferase-2 is expressed in spermatic germ cells and incorporates arachidonic acid into triacylglycerols, PLoS One 7 (2012) e42986. [PubMed: 22905194]

[6]. Cao J, Li JL, Li D, Tobin JF, Gimeno RE, Molecular identification of microsomal acyl-CoA: glycerol-3-phosphate acyltransferase, a key enzyme in de novo triacylglycerol synthesis, Proc. Natl. Acad. Sci. U. S. A 103 (2006) 19695–19700. [PubMed: 17170135]

[7]. Cao J, Perez S, Goodwin B, Lin Q, Peng H, Qadri A, Zhou Y, Clark RW, Perreault M, Tobin JF, Gimeno RE, Mice deleted for GPAT3 have reduced GPAT activity in white adipose tissue and altered energy and cholesterol homeostasis in diet-induced obesity, Am. J. Physiol. Endocrinol. Metab 306 (2014) 1176–1187.

[8]. Cooper DE, Grevengoed TJ, Klett EL, Coleman RA, Glycerol-3-phosphate acyltransferase isoform-4 (GPAT4) limits oxidation of exogenous fatty acids in brown adipocytes, J. Biol. Chem 290 (2015) 15112–15120. [PubMed: 25918168]

[9]. Megias A, Municio AM, Perez-Albarsanz MA, Biochemistry of development in insects. Triacyglycerol and phosphoglyceride biosynthesis by subcellular fractions, Eur. J. Biochem 72 (1977)9–16. [PubMed: 836395]

[10]. Canavoso LE, Wells MA, Metabolic pathways for diacylglycerol biosynthesis and release in the midgut of larval Manduca sexta, Insect Biochem. Mol. Biol 30 (2000) 1173–1180. [PubMed: 11044663]

[11]. Du M, Liu X, Liu X, Yin X, Han S, Song Q, An S, Glycerol-3-phosphateO-acyltransferase is required for PBAN-induced sex pheromone biosynthesis in Bombyx mori, Sci. Rep 5 (2015) 8110. [PubMed: 25630665]

[12]. Pellon-Maison M, Garcia CF, Cattaneo ER, Coleman RA, Gonzalez-Baro MR, Macrobrachium borellii hepatopancreas contains a mitochondrial glycerol-3-phosphate acyltransferase which initiates triacylglycerol biosynthesis, Lipids 44 (2009) 337–344. [PubMed: 19130111]

[13]. Tian Y, Bi J, Shui G, Liu Z, Xiang Y, Liu Y, Wenk MR, Yang H, Huang X, Tissue-autonomous function of Drosophila seipin in preventing ectopic lipid droplet formation, PLoS Genet. 7 (2011) e1001364. [PubMed: 21533227]

[14]. Kühnlein RP, Thematic review series: lipid droplet synthesis and metabolism: from yeast to man. Lipid droplet-based storage fat metabolism in Drosophila, J. Lipid Res 53 (2012) 1430–1436. [PubMed: 22566574]

[15]. Wilfling F, Wang H, Haas JT, Krahmer N, Gould TJ, Uchida A, Cheng JX, Graham M, Christiano R, Fröhlich F, Liu X, Buhman KK, Coleman RA, Bewersdorf J, Farese RVJ, Walther TC, Triacylglycerol synthesis enzymes mediate lipid droplet growth by relocalizing from the ER to lipid droplets, Dev. Cell 24 (2013) 383–399.

[16]. Pontes EG, Leite P, Majerowicz D, Atella GC, Gondim KC, Dynamics of lipid accumulation by the fat body of Rhodnius prolixus: the involvement of lipophorin binding sites, J. Insect Physiol 54 (2008) 790–797. [PubMed: 18395740]

[17]. Alves-Bezerra M, De Paula IF, Medina JM, Silva-Oliveira G, Medeiros JS, Gäde G, Gondim KC, Adipokinetic hormone receptor gene identification and its role in triacylglycerol metabolism in the blood-sucking insect Rhodnius prolixus, Insect Biochem. Mol. Biol 69 (2016) 51–60. [PubMed: 26163435]

[18]. Alves-Bezerra M, Gondim KC, Triacylglycerol biosynthesis occurs via the glycerol3-phosphate pathway in the insect Rhodnius prolixus, Biochim. Biophys. Acta 1821 (2012) 1462–1471. [PubMed: 22902317]

[19]. Mesquita RD, Seabra-Junior ES, in: INPI (Ed.), FAT (Functional Analysis Tool), 2011 (Brazil).

[20]. Nakai K, Horton P, PSORT: a program for detecting sorting signals in proteins and predicting their subcellular localization, Trends Biochem. Sci 24 (1999) 34–36. [PubMed: 10087920]

[21]. Alves-Bezerra M, Klett EL, De Paula IF, Ramos IB, Coleman RA, Gondim KC, Long-chain acyl-CoA synthetase 2 knockdown leads to decreased fatty acid oxidation in fat body and reduced reproductive capacity in the insect Rhodnius prolixus, Biochim. Biophys. Acta 1861 (2016) 650–662. [PubMed: 27091636]

[22]. Majerowicz D, Alves-Bezerra M, Logullo R, Fonseca-de-Souza AL, Meyer-Fernandes JR, Braz GR, Gondim KC, Looking for reference genes for real-time quantitative PCR experiments in Rhodnius prolixus (Hemiptera: Reduviidae), Insect Mol. Biol 20 (2011) 713–722. [PubMed: 21929722]

[23]. Rasmussen R, Quantification on the LightCycler, in: Meuer S, Wittwer C, Nakagawa K. (Eds.), Rapid Cycle Real-time PCR, methods and applications, Springer Press 2001, pp. 21–34.

[24]. Bustin SA, Benes V, Garson JA, Hellemans J, Huggett J, Kubista M, Mueller R, Nolan T, Pfaffl MW, Shipley GL, Vandesompele J, Wittwer CT, The MIQE guidelines: minimum information for publication of quantitative real-time PCR experiments, Clin. Chem 55 (2009) 611–622. [PubMed: 19246619]

[25]. Chang YYK, Kennedy EP, Biosynthesis of phosphatidyl glycerophosphate in Escherichia coli, J. Lipid Res 8 (1967) 447–455. [PubMed: 4860577]

[26]. Coleman RA, Haynes EB, Selective changes in microsomal enzymes of triacylglycerol and phosphatidylcholine synthesis in fetal and postnatal rat liver: induction of microsomal sn-glycerol 3-P and dihydroxyacetone-P acyltransferase activities, J. Biol. Chem 258 (1983) 450–456. [PubMed: 6848513]

[27]. Schlossman DM, Bell RM, Triacylglycerol synthesis in isolated fat cells. Evidence that the sn-glycerol-3-phosphate and dihydroxyacetone phosphate acyltransferase activities are dual catalytic functions of a single microsomal enzyme, J. Biol. Chem 251 (1976) 5738–5744. [PubMed: 9398]

[28]. Naito Y, Yamada T, Matsumiya T, Ui-Tei K, Saigo K, Morishita S, dsCheck: highly sensitive off-target search software for double-stranded RNA-mediated RNA interference, Nucleic Acids Res. 33 (2005) W589–W591. [PubMed: 15980542]

[29]. Hansen IA, Attardo GM, Roy SG, Raikhel AS, Target of rapamycin-dependent activation of S6 kinase is a central step in the transduction of nutritional signals during egg development in a mosquito, J. Biol. Chem 280 (2005) 20565–20572. [PubMed: 15788394]

[30]. Bligh EG, Dyer WJ, A rapid method of total lipid extraction and purification, Can. J. Biochem. Physiol 37 (1959) 911–917. [PubMed: 13671378]

[31]. Gondim KC, Oliveira PL, Coelho HSL, Masuda H, Lipophorin from Rhodnius prolixus: purification and partial characterization, Insect Biochem. 19 (1989) 153–161.

[32]. Coelho HSL, Atella GC, Moreira MF, Gondim KC, Masuda H, Lipophorin density variation during oogenesis inRhodnius prolixus, Arch. Insect Biochem. Physiol 35 (1997) 301–313. [PubMed: 9177134]

[33]. Fan Y, Schal C, Vargo EL, Bagnères AG, Characterization of termite lipophorin and its involvement in hydrocarbon transport, J. Insect Physiol 50 (2004) 609–620. [PubMed: 15234621]

[34]. Horwitz J, Perlman RL, Phospholipid metabolism in PC12 pheochromocytoma cells, Methods Enzymol. 141 (1977) 169–175.

[35]. Bitman J, Wood DL, An improved copper reagent for quantitative densitometric thin-layer chromatography of lipids, J. Liq. Chromatogr 5 (1982) 1155–1162.

[36]. Defferrari MS, Orchard I, Lange AB, Identification of thefirst insulin-like peptide in the disease vector Rhodnius prolixus:involvement in metabolic homeostasis of lipids and carbohydrates, Insect Biochem. Mol. Biol 70 (2016) 148–159. [PubMed: 26742603]

[37]. Daims H, Lücker S, Wagner M, daime, a novel image analysis program for microbial ecology and biofilm research, Environ. Microbiol 8 (2006) 200–213. [PubMed: 16423009]

[38]. Burns MJ, Nixon GJ, Foy CA, Harris N, Standardisation of data from real-time quantitative PCR methods–evaluation of outliers and comparison of calibration curves, BMC Biotechnol. 5 (2005) 31. [PubMed: 16336641]

[39]. Lewin TM, Wang P, Coleman RA, Analysis of amino acid motifs diagnostic for the sn-glycerol-3-phosphate acyltransferase reaction, Biochemistry 38 (1999) 5764–5771. [PubMed: 10231527]

[40]. Coleman RA, Lee DP, Enzymes of triacylglycerol synthesis and their regulation, Prog. Lipid Res 43 (2004) 134–176. [PubMed: 14654091]

[41]. Takeuchi K, Reue K, Biochemistry, physiology, and genetics of GPAT, AGPAT, and lipin enzymes in triglyceride synthesis, Am. J. Physiol. Endocrinol. Metab 296 (2009) E1195–E1209. [PubMed: 19336658]

[42]. Grillo LAM, Majerowicz D, Gondim KC, Lipid metabolism in Rhodnius prolixus (Hemiptera: Reduviidae): role of a midgut triacylglycerol-lipase, Insect Biochem. Mol. Biol 37 (2007) 579–588. [PubMed: 17517335]

[43]. Atella GC, Gondim KC, Masuda H, Loadingoflipophorin particles with phospholipids at the midgut of Rhodnius prolixus, Arch. Insect Biochem. Physiol 30 (1995) 337–350. [PubMed: 11488302]

[44]. Stapleton CM, Mashek DG, Wang S, Nagle CA, Cline GW, Thuillier P, Leesnitzer LM, Li LO, Stimmel JB, Shulman GI, Coleman RA, Lysophosphatidic acid activates peroxisome proliferator activated receptor-γ in CHO cells that over-express glycerol 3-phosphate acyltransferase-1, PLoS One 6 (2011) e18932. [PubMed: 21533082]

[45]. Jump DB, Tripathy S, Depner CM, Fatty acid-regulated transcription factors in the liver, Annu. Rev. Nutr 33 (2013) 249–269. [PubMed: 23528177]

[46]. Nakamura MT, Yudell BE, Loor JJ, Regulation of energy metabolism by long-chain fatty acids, Prog. Lipid Res (2014) 53124–53144.

[47]. Shapiro JP, Wells MA, Law JH, Lipid transport in insects, Annu. Rev. Entomol 33 (1988) 297–318. [PubMed: 3277529]

[48]. Santos R, Rosas-Oliveira R, Saraiva FB, Majerowicz D, Gondim KC, Lipid accumulation and utilization by oocytes and eggs of Rhodnius prolixus, Arch. Insect Biochem. Physiol 77 (2011)1–16. [PubMed: 21308762]

[49]. Arrese EL, Soulages JL, Insect fat body: energy, metabolism, and regulation, Annu. Rev. Entomol 55 (2010) 207–225. [PubMed: 19725772]

[50]. Guo Y, Walther TC, Rao M, Stuurman N, Goshima G, Terayama K, Wong JS, Vale RD, Walter P, Farese RV, Functional genomic screen reveals genes involved in lipid-droplet formation and utilization, Nature 453 (2008) 657–661. [PubMed: 18408709]

[51]. Hammond LE, Gallagher PA, Wang SL, Hiller S, Kluckman KD, Posey-Marcos EL, Maeda N, Coleman RA, Mitochondrial glycerol-3-phosphate acyltransferase-deficient mice have reduced

weight and liver triacylglycerol content and altered glycerolipid fatty acid composition, Mol. Cell. Biol 22 (2002) 8204–8214. [PubMed: 12417724]

[52]. Hammond LE, Neschen S, Romanelli AJ, Cline GW, Ilkayeva OR, Shulman GI, Muoio DM, Coleman RA, Mitochondrial glycerol-3-phosphate acyltransferase-1 is essential in liver for the metabolism of excess acyl-CoAs, J. Biol. Chem 280 (2005) 25629–25636. [PubMed: 15878874]

[53]. Mesquita RD, Vionette-Amaral RJ, Lowenberger C, Rivera-Pomar R, Monteiro FA, Minx P, Spieth J, Carvalho AB, Panzera F, Lawson D, Torres AQ, Ribeiro JM, Sorgine MH, Waterhouse RM, Montague MJ, Abad-Franch F, Alves-Bezerra M, Amaral LR, Araujo HM, Araujo RN, Aravind L, Atella GC, Azambuja P, Berni M, Bittencourt-Cunha PR, Braz GR, Calderón-Fernández G, Carareto CM, Christensen MB, Costa IR, Costa SG, Dansa M, Daumas-Filho CR, De-Paula IF, Dias FA, Dimopoulos G, Emrich SJ, Esponda-Behrens N, Fampa P, Fernandez-Medina RD, da Fonseca RN, Fontenele M, Fronick C, Fulton LA, Gandara AC, Garcia ES, Genta FA, Giraldo-Calderón GI, Gomes B, Gondim KC, Granzotto A, Guarneri AA, Guigó R, Harry M, Hughes DS, Jablonka W, Jacquin-Joly E, Juárez MP, Koerich LB, Latorre-Estivalis JM, Lavore A, Lawrence GG, Lazoski C, Lazzari CR, Lopes RR, Lorenzo MG, Lugon MD, Majerowicz D, Marcet PL, Mariotti M, Masuda H, Megy K, Melo AC, Missirlis F, Mota T, Noriega FG, Nouzova M, Nunes RD, Oliveira RL, Oliveira-Silveira G, Ons S, Pagola L, Paiva-Silva GO, Pascual A, Pavan MG, Pedrini N, Peixoto AA, Pereira MH, Pike A, Polycarpo C, Prosdocimi F, Ribeiro-Rodrigues R, Robertson HM, Salerno AP, Salmon D, Santesmasses D, Schama R, Seabra-Junior ES, Silva-Cardoso L, Silva-Neto MA, Souza-Gomes M, Sterkel M, Taracena ML, Tojo M, Tu ZJ, Tubio JM, Ursic-Bedoya R, Venancio TM, Walter-Nuno AB, Wilson D, Warren WC, Wilson RK, Huebner E, Dotson EM, Oliveira PL, Genome ofRhodnius prolixus, an insect vector of Chagas disease, reveals unique adaptations to hematophagy and parasite infection, Proc. Natl. Acad. Sci. U. S. A 112 (2015) 14936–14941. [PubMed: 26627243]

[54]. Shan DD, Li JL, Wu LY, Li DM, Hurov J, Tobin JF, Gimeno RE, Cao JS, GPAT3 and GPAT4 are regulated by insulin-stimulated phosphorylation and play distinct roles in adipogenesis, J. Lipid Res 51 (2010) 1971–1981. [PubMed: 20181984]

[55]. Lewin TM, Granger DA, Kim JH, Coleman RA, Regulation of mitochondrial sn-glycerol-3-phosphate acyltransferase activity: response to feeding status is unique in various rat tissues and is discordant with protein expression, Arch. Biochem. Biophys 396 (2001) 119–127. [PubMed: 11716470]

[56]. Onorato TM, Chakraborty S, Haldar D, Phosphorylation of rat liver mitochondrial glycerol-3-phosphate acyltransferase by casein kinase 2, J. Biol. Chem 280 (2005) 19527–19534. [PubMed: 15778226]

[57]. Muoio DM, Seefeld K, Witters LA, Coleman RA, AMP-activated kinase reciprocally regulates triacylglycerol synthesis and fatty acid oxidation in liver and muscle: evidence that sn-glycerol-3-phosphate acyltransferase is a novel target, Biochem. J338 (1999) 783–791. [PubMed: 10051453]

[58]. Nimmo HG, Houston B, Rat adipose-tissue glycerol phosphate acyltransferase can be inactivated by cyclic AMP-dependent protein kinase, Biochem. J 176 (1978) 607–610. [PubMed: 217367]

[59]. Zhang C, Wendel AA, Keogh MR, Harris TE, Chen J, Coleman RA, Glycerolipid signals alter mTOR complex 2 (mTORC2) to diminish insulin signaling, Proc. Natl. Acad. Sci. U. S. A 109 (2012) 1667–1672. [PubMed: 22307628]

[60]. Zhang C, Cooper DE, Grevengoed TJ, Li LO, Klett EL, Eaton JM, Harris TE, Coleman RA, Glycerol-3-phosphate acyltransferase-4-deficient mice are protected from diet-induced insulin resistance by the enhanced association of mTOR and rictor, Am. J. Physiol. Endocrinol. Metab 307 (3) (2014) E305–E315. [PubMed: 24939733]

[61]. McIntyre TM, Pontsler AV, Silva AR, St Hilaire A, Xu Y, Hinshaw JC, Zimmerman GA, Hama K, Aoki J, Arai H, Prestwich GD, Identification of an intracellular receptor for lysophosphatidic acid (LPA): LPA is a transcellular PPAR gamma agonist, Proc. Natl. Acad. Sci. U. S. A 100 (2003) 131–136. [PubMed: 12502787]

[62]. Majerowicz D, Hannibal-Bach HK, Castro RS, Bozaquel-Morais BL, Alves-Bezerra M, Grillo LA, Masuda CA, Færgeman NJ, Knudsen J, Gondim KC, The ACBP gene family in Rhodnius prolixus:expression, characterization and function of RpACBP-1, Insect Biochem. Mol. Biol 72 (2016).

[63]. Linden D, William-Olsson L, Rhedin M, Asztely AK, Clapham JC, Schreyer S, Overexpression of mitochondrial GPAT in rat hepatocytes leads to decreased fatty acid oxidation and increased glycerolipid biosynthesis, J. Lipid Res 45 (2004) 1279–1288. [PubMed: 15102885]

[64]. Lewin TM, Wang SL, Nagle CA, Van Horn CG, Coleman RA, Mitochondrial glycerol-3-phosphate acyltransferase-1 directs the metabolic fate of exogenous fatty acids in hepatocytes, Am. J. Physiol. Endocrinol. Metab 288 (2005) E835–E844. [PubMed: 15598672]

[65]. Linden D, William-Olsson L, Ahnmark A, Ekroos K, Hallberg C, Sjogren HP, Becker B, Svensson L, Clapham JC, Oscarsson J, Schreyer S, Liver-directed overexpression of mitochondrial glycerol-3-phosphate acyltransferase results in hepatic steatosis, increased triacylglycerol secretion and reduced fatty acid oxidation, FASEB J. 20 (2006) 434–443. [PubMed: 16507761]

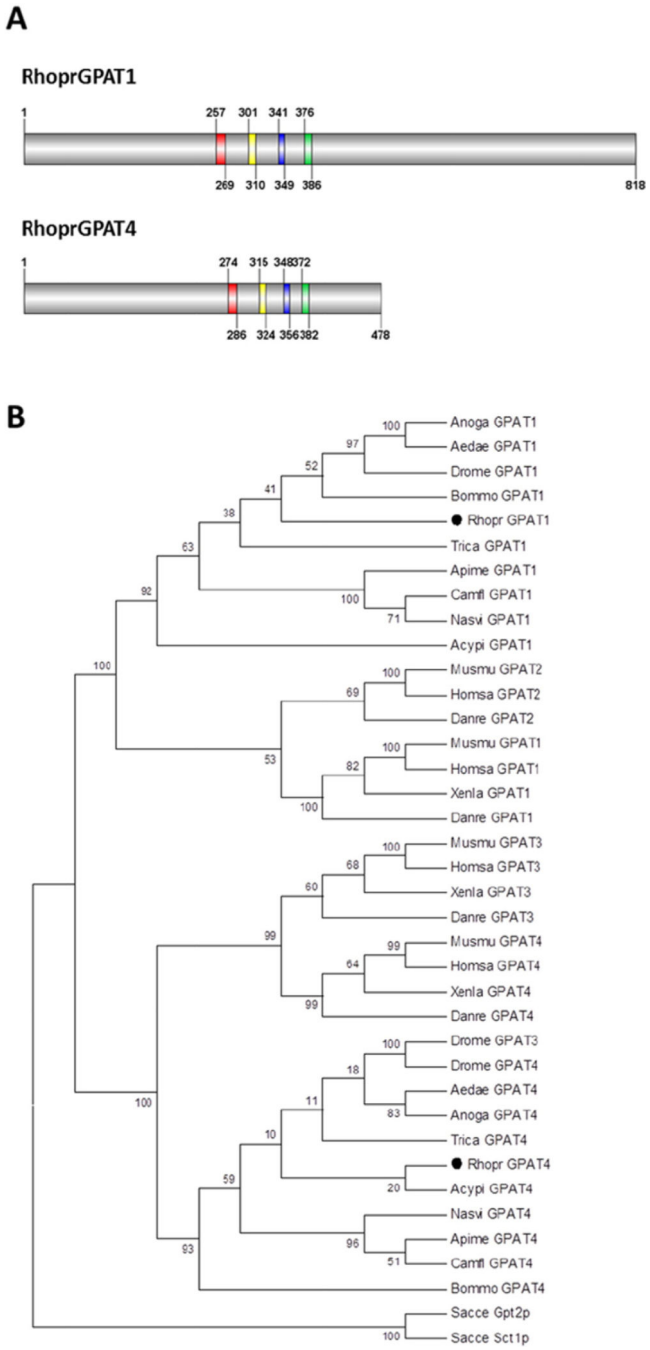

Fig. 1.

Domain structure and phylogenetic analysis of GPAT proteins. (A) *R. prolixus* GPAT proteins. Red, yellow, blue and green boxes, motifs I–IV, respectively. Numbers indicate amino acid positions. (B) Amino acid sequences of GPAT from different organisms (38 taxa) were aligned and the dendrogram was constructed using MEGA 4.0 software with the Maximum Parsimony algorithm and a Bootstrap of 1000 replications. All positions containing gaps and missing data were eliminated from the dataset (Complete Deletion option). The final dataset contained 333 informative positions. The numbers at the

branching points are Bootstrap values. The accession numbers of the protein sequences used in these analyses are presented in Supplementary Table 2. Acypi, *Acyrthosiphon pisum*; Aedae, *Aedes aegypti*; Anoga, *Anopheles gambiae*; Apime, *Apis melífera*; Bommo, *Bombyx mori*; Camfl, *Camponotus floridanus*; Danre, *Danio rerio*; Drome, *Drosophila melanogaster*; Homsa, *Homo sapiens*; Musmu, *Mus musculus*; Nasvi, *Nasonia vitripennis*; Rhopr, *Rhodnius prolixus*; Sacce, *Saccharomyces cerevisiae*; Trica, *Tribolium castaneum*; Xenla, *Xenopus laevis*.

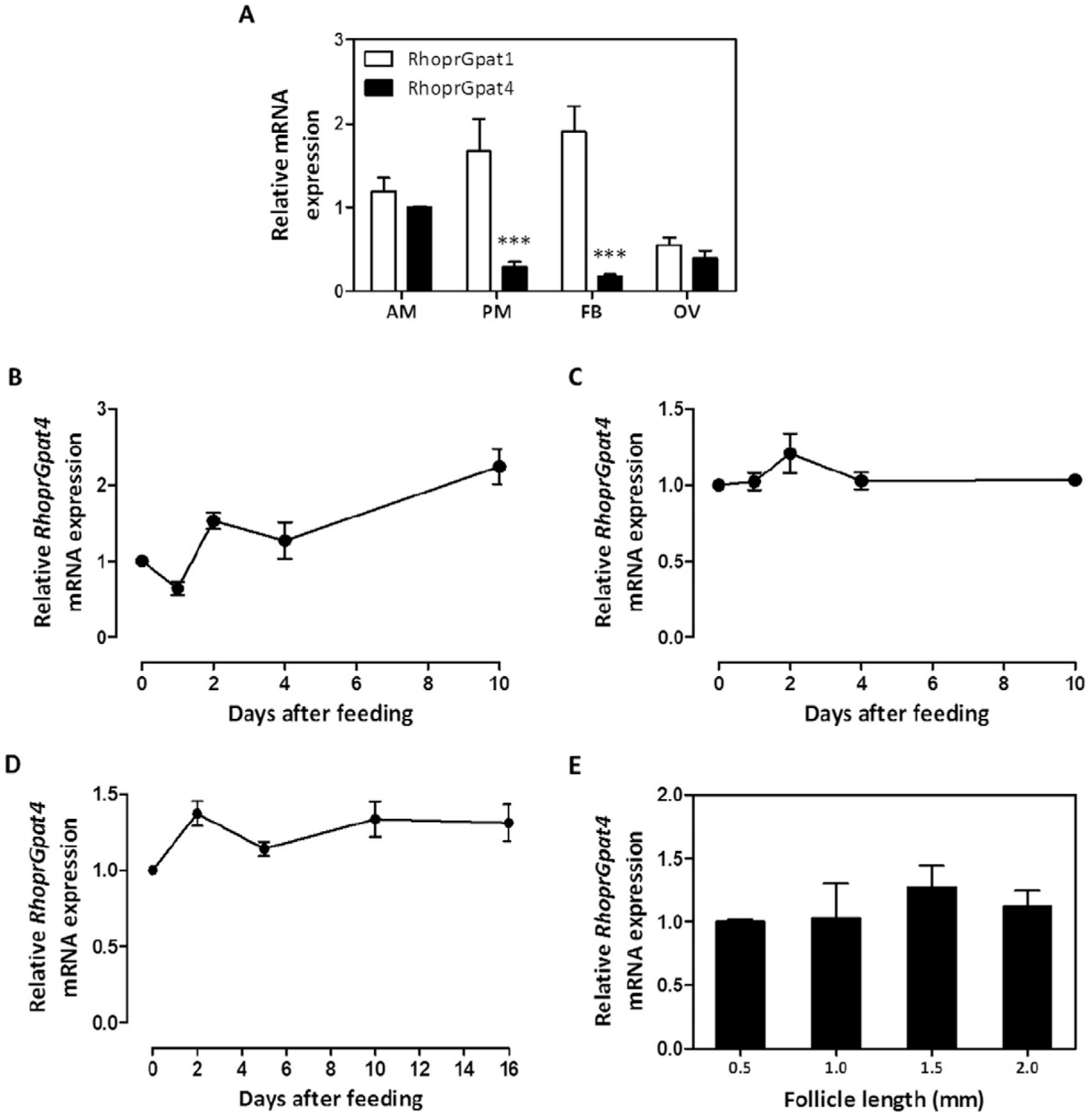

Fig. 2.

RhoprGpat1 and *RhoprGpat4* are differentially expressed. At the fourth day after blood meal, anterior midgut (AM), posterior midgut (PM), fat body (FB) and ovary (OV) were dissected from adult females and *RhoprGpat1* and *RhoprGpat4* mRNA expression levels were determined by qPCR (A). Alternatively, anterior midgut (B), posterior midgut (C) and fat body (D) were obtained from adult females before feeding (day 0) or on different days after blood meal. Follicles of different lengths (E) were isolated from females on day 4 after a blood meal. Differences between *RhoprGpat4* cDNA levels were determined by qPCR

analysis. mRNA expression levels are relative to *RhoprGpat4* transcripts in the anterior midgut (A), in unfed insects (B–D) or 0.5 mm follicles (E), set as 1.0. The results represent the means ± S.E.M. of 3–4 independent experiments. Where not seen, error bars are smaller than the symbols. (***): $P < 0.001$ compared to *RhoprGpat1* values by one-way ANOVA.

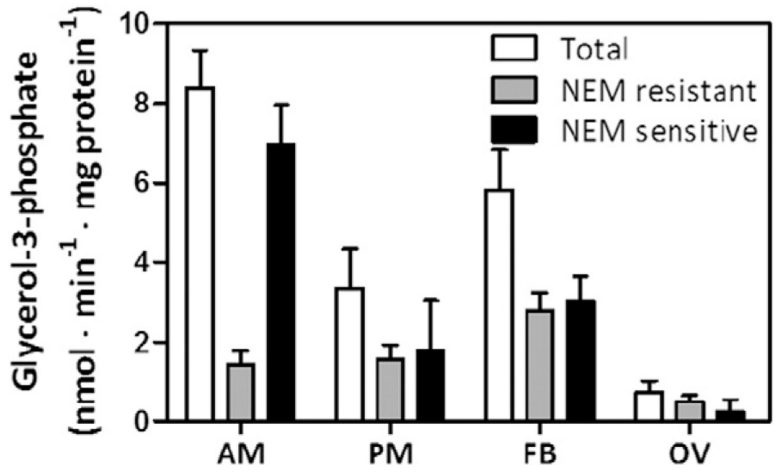

Fig. 3.

RhoprGPAT1 and RhoprGPAT4 have differential activity among tissues. Anterior and posterior midgut, fat body and ovary were obtained from adult females four days after blood feeding. Cellular membranes were isolated and samples (4–8 μg) were assayed for GPAT activity. Total, *N*-ethylmaleimide (NEM) resistant, and NEM sensitive GPAT specific activity were determined. The results represent the means ± S.E.M. (n = 4 biological replicates in 2 assay runs). AM: anterior midgut; PM: posterior midgut; FB: fat body; OV: ovary.

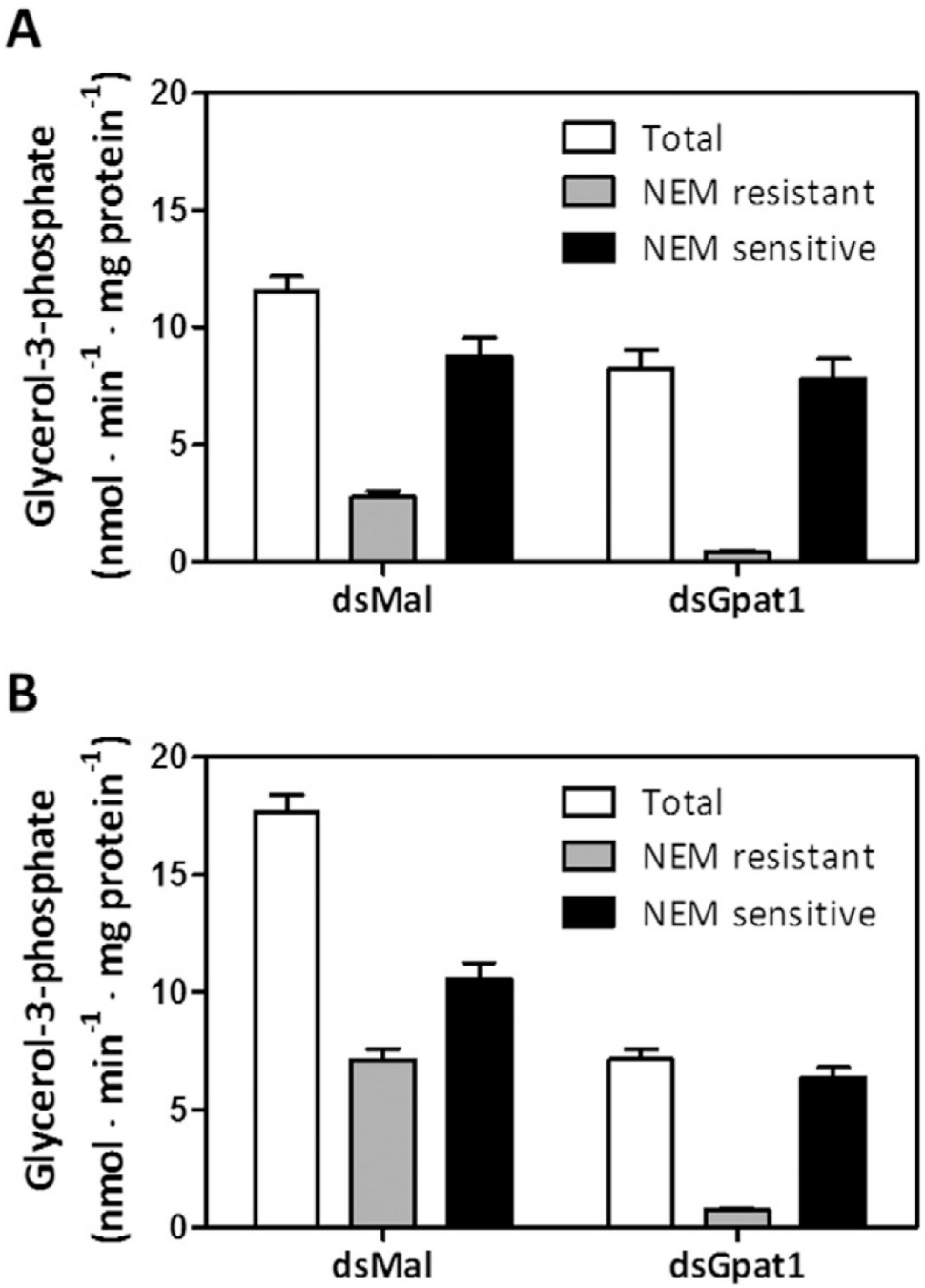

Fig. 4.

RhoprGpat1 knockdown reduces NEM resistant GPAT activity. Fasted adult females were injected with dsRNA for *RhoprGpat1* or *Mal* (control) genes. Insects were fed on the third day after injection. Midgut (anterior and posterior portions) (A) and fat body (B) were obtained on the 2nd and 5th day after feeding, respectively. Cellular membranes were isolated and samples (4–8 μg) were assayed for GPAT activity. Total, *N*-ethylmaleimide (NEM) resistant, and NEM sensitive GPAT specific activity were determined. The results represent the means ± S.E.M. (n = 3 biological replicates in 2 assay runs).

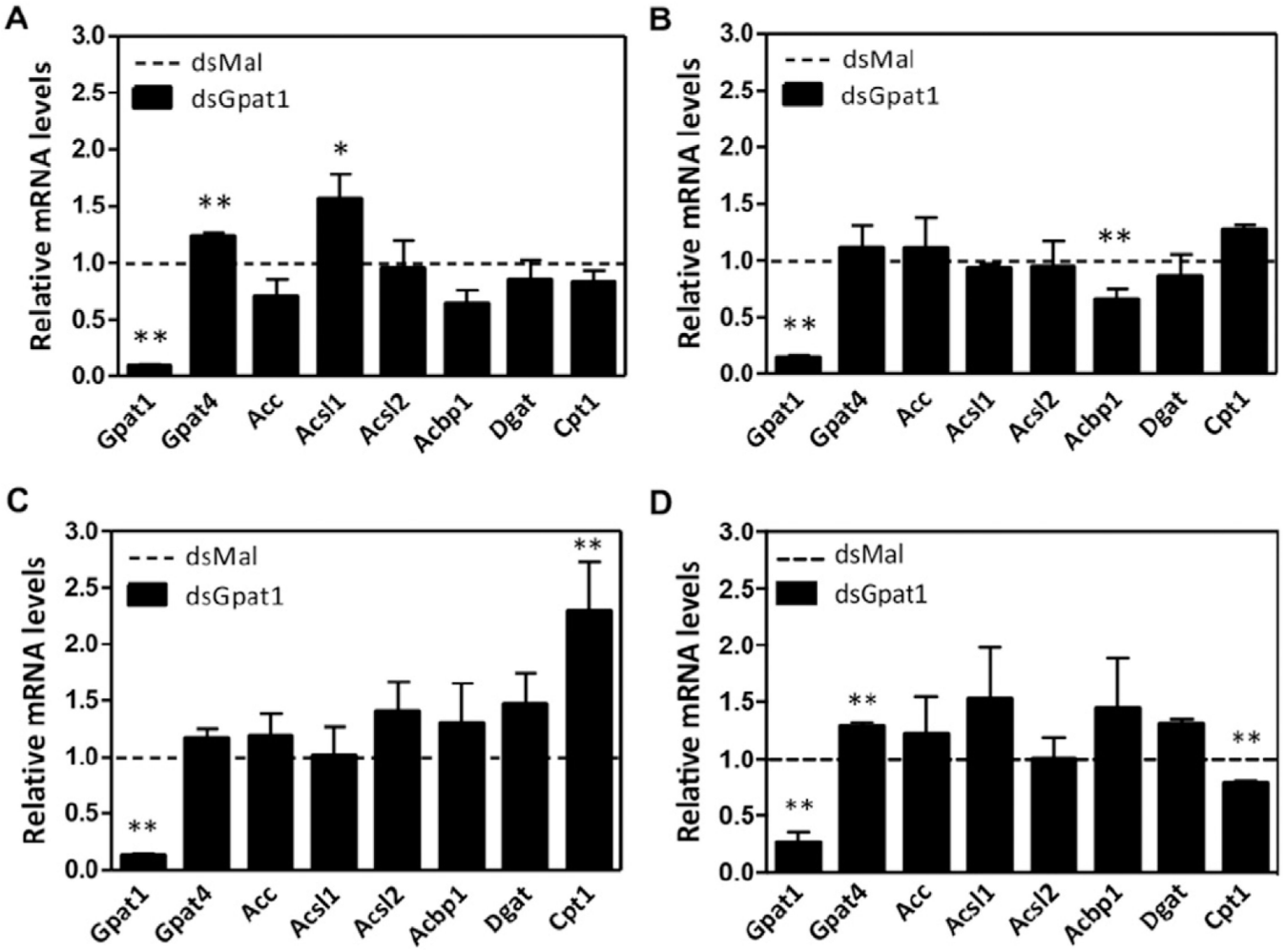

Fig. 5.

Effect of *RhoprGpat1* knockdown on the expression of lipid-related genes. Fasted adult females were injected with dsRNA for *RhoprGpat1* or *Mal* (control) genes. Insects were fed on the third day after injection. Anterior (A) and posterior (B) midguts were obtained on the 2nd day after feeding. Fat body (C) and ovary (D) were obtained on the 5th day after feeding. Differences between cDNA levels were determined by qPCR analysis. mRNA expression levels are relative to those from control insects (dashed lines). The results represent the means ± S.E.M. of 4 independent experiments. (*) and (**): $P <$ 0.05 and P b 0.01, respectively, compared to reference values by Student's *t*-test. *Gpat1*: glycerol-3-phosphate acyltransferase 1; *Gpat4*: glycerol-3-phosphate acyltransferase 1; *Acc*: acetyl-CoA carboxylase; *Acsl1*: long-chain acyl-CoA synthetase 1; *Acsl2*: long-chain acyl-CoA synthetase 1; Acbp1: acyl-CoA-binding protein 1; *Dgat*: diacylglycerol acyltransferase; *Cpt1:* carnitine palmitoyltransferase 1.

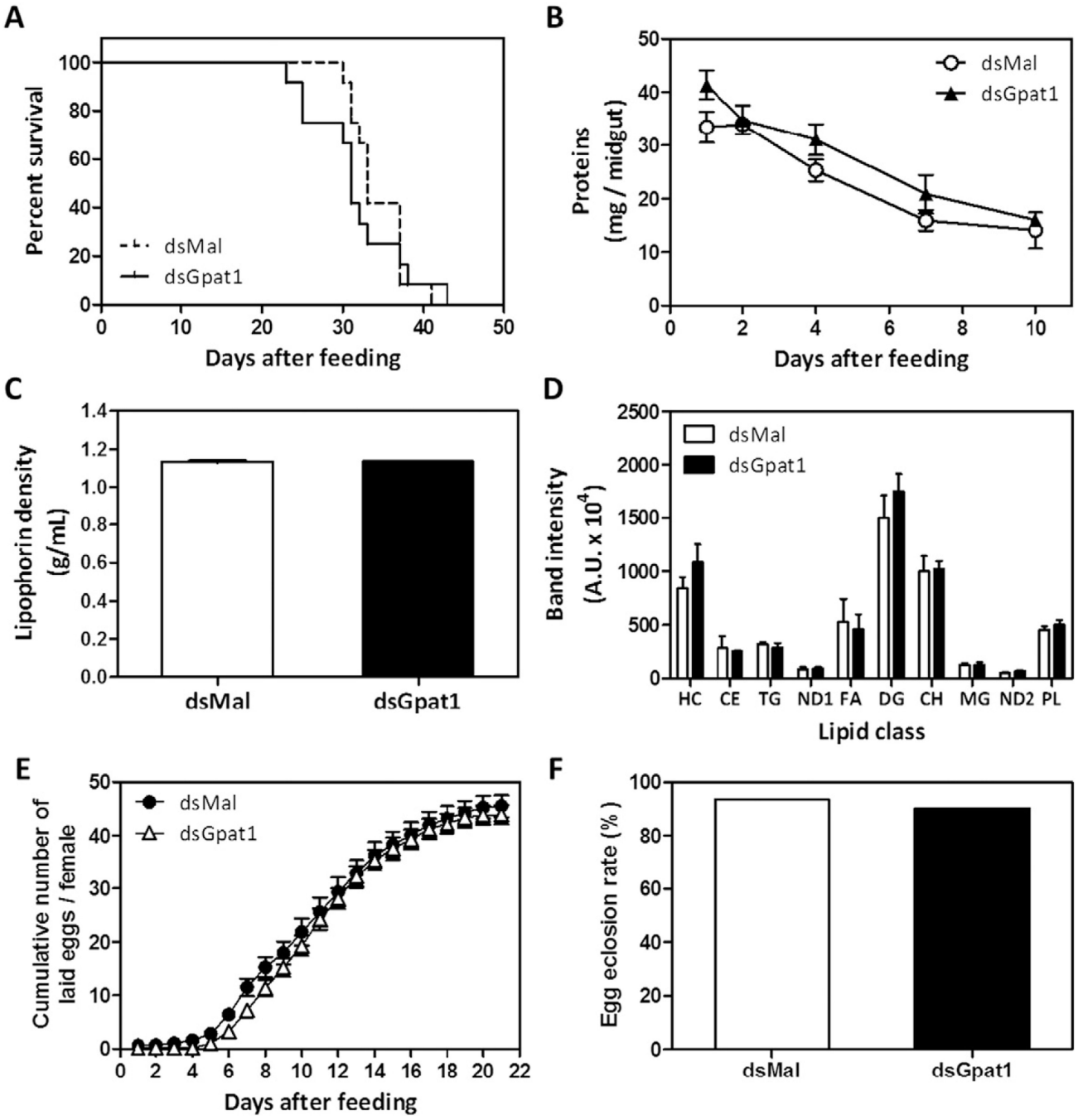

Fig. 6.

Lifespan, digestion, circulating lipids, and oviposition are not affected by *RhoprGpat1* knockdown. Fasted adult females were injected with dsRNA for *RhoprGpat1* or Mal (control) genes. Insects were fedon the third day after injection. (A) Insect mortality was followed (n= 12 insects, in 2 independent experiments). (B) The amount of total protein in the midgut was determined at different days after the blood meal. Results are means ± S.E.M. (n = 8 insects in 3 independent experiments). (C) Hemolymph was collected on the 4th day after feeding and lipophorin density was determined. Alternatively, lipid

composition of hemolymph was determined by TLC (D). Results are means ± S.E.M., n = 3 independent experiments. HC: hydrocarbon; CE: cholesteryl ester; TG: triacylglycerol; ND: not determined; FA, fatty acid; DG, diacylglycerol; CH, cholesterol; MG, monoacylglycerol; PL: phospholipid. (E) Cumulative oviposition was followed. Results are means ± S.E.M., n = 22 insects, in 4 independent experiments. (F) The eggs were collected after oviposition and the egg hatching percentage was determined (n ≥ 460 eggs, in 2 independent experiments).

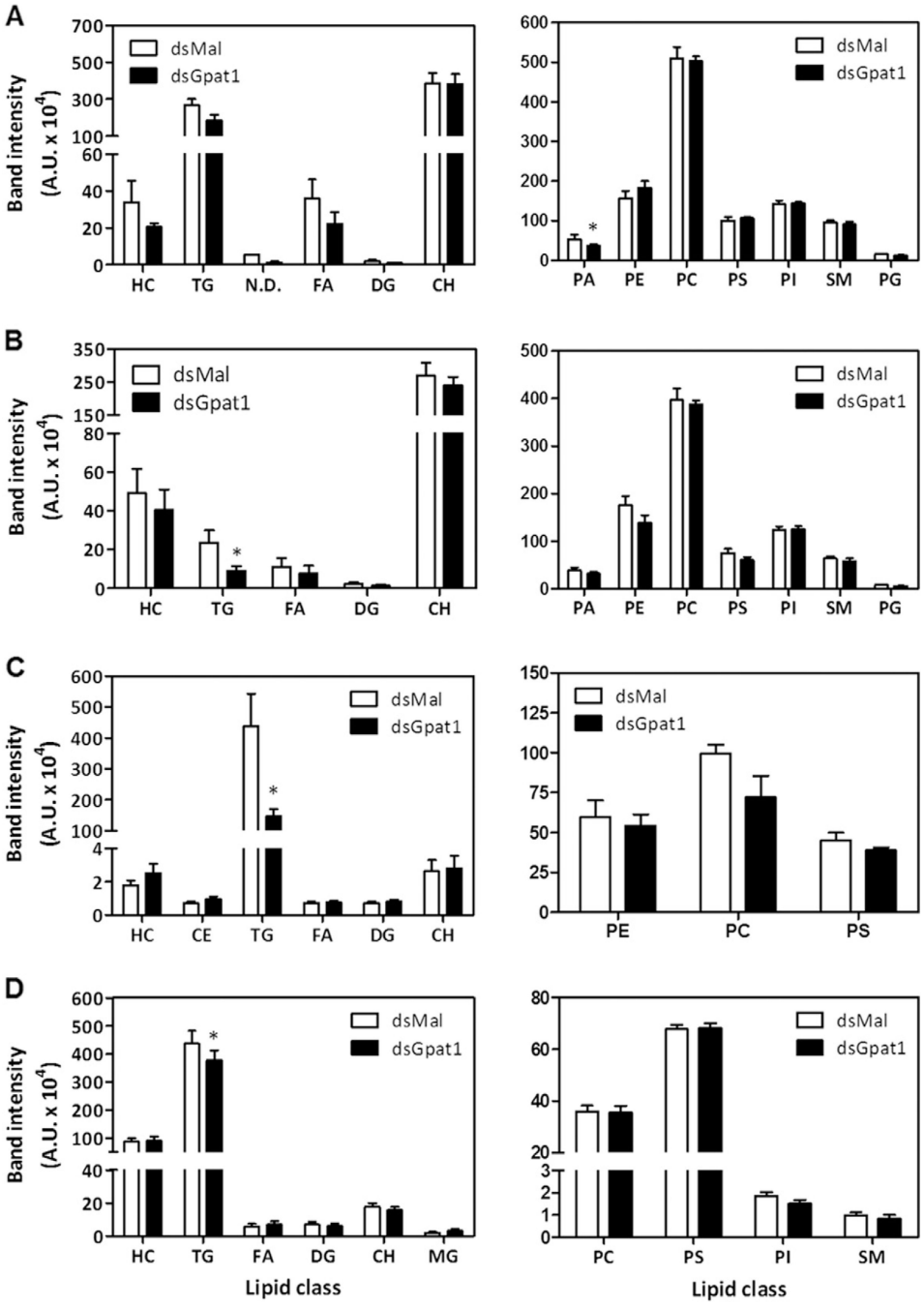

Fig. 7.

RhoprGpat1 knockdown reduces TAG content in the posterior midgut and fat body. Fasted adult females were injected with dsRNA for *RhoprGpat1* or *Mal* (control) genes. Insects were fed on the third day after injection. Anterior midgut (A) and posterior midgut (B) were dissected on the 2nd day after feeding. Fat body (C) and laid eggs (D) were obtained on the 5th day after feeding. The composition of neutral lipids (left panels) and phospholipids (right panels) were determined by TLC. Results are means ± S.E.M., n = 3 independent experiments. (*): $P < 0.05$ compared to control values by

Student's *t*-test. CH, cholesterol; DG, diacylglycerol; FA, fatty acid; HC, hydrocarbon; MG, monoacylglycerol; N.D., not determined; PA, phosphatidic acid; PC, phosphatidylcholine; PE, phosphatidylethanolamine; PG, phosphatidylglycerol; PI, phosphatidylinositol; PS, phosphatidylserine; SM, sphingomyelin; TG, triacylglycerol.

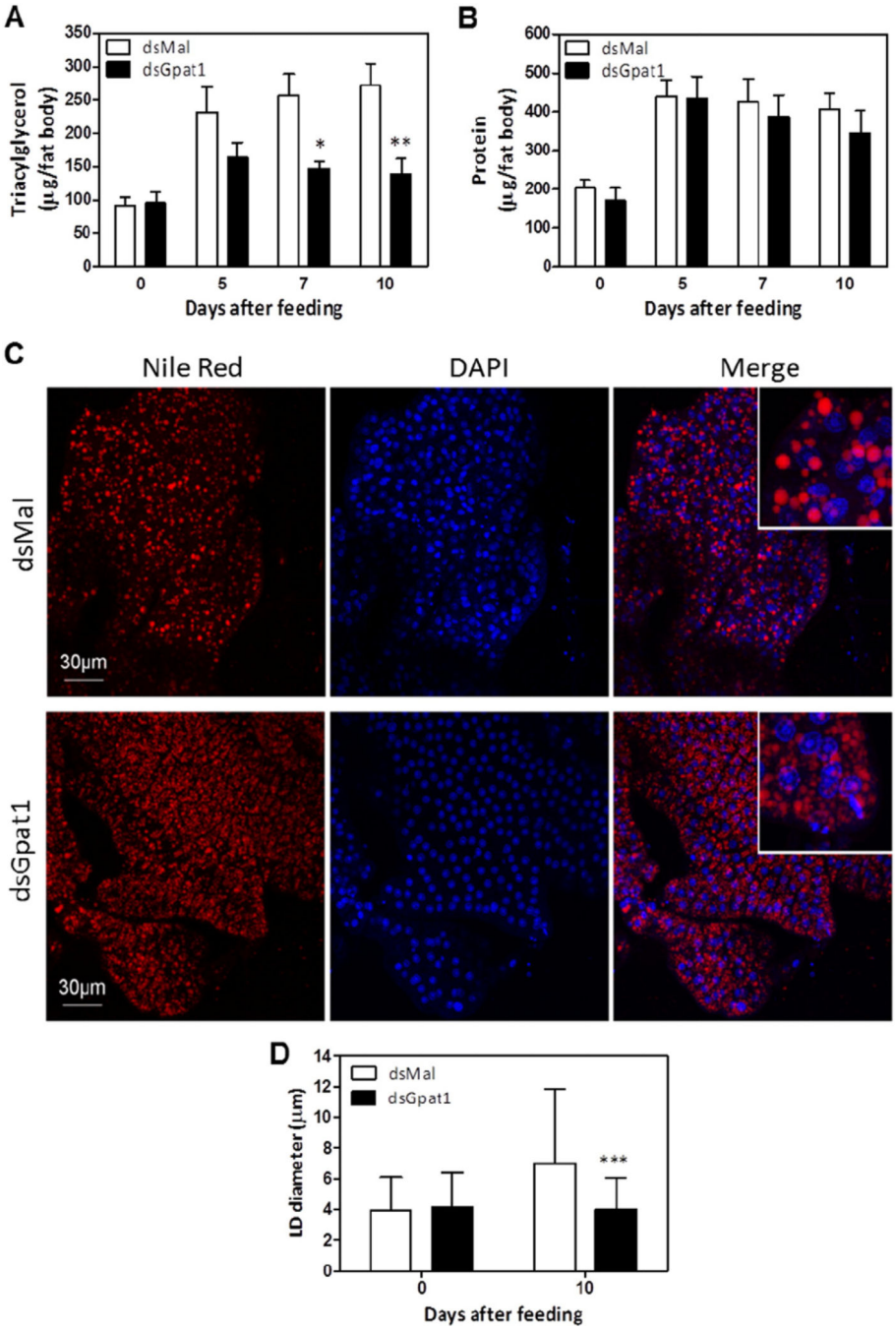

Fig. 8.

TAG accumulation after feeding is dependent on RhoprGPAT1. Fasted adult females were injected with dsRNA for *RhoprGpat1* or *Mal* (control) genes. Insects were fed on the third day after injection. Insects were dissected before feeding (day 0) or at different days after the blood meal. The amount of triacylglycerol (A) and protein (B) was determined in the fat body. Results are means ± S.E.M., n = 9–12 insects, in 3 independent experiments. (*) and (**): $P < 0.05$ and $P < 0.01$, respectively, when compared to control values by two-way ANOVA. Nile Red stained-lipid droplets and DAPI-stained nuclei were imaged

from optical sections of fat bodies dissected from control and *RhoprGpat1*-silenced females before feeding (day 0) or on the 10th day after feeding. (C) Representative images from fat bodies on the 10th day after feeding. Scale bars = 30 μm. (D) The average lipid droplet diameter was determined from the images shown in panel C (10th day after blood meal) and in Supplementary Fig. 2 (day 0). Results are means ± S.D., from at least 500 lipid droplets. (***): $P < 0.001$ when compared to control by two-way ANOVA.

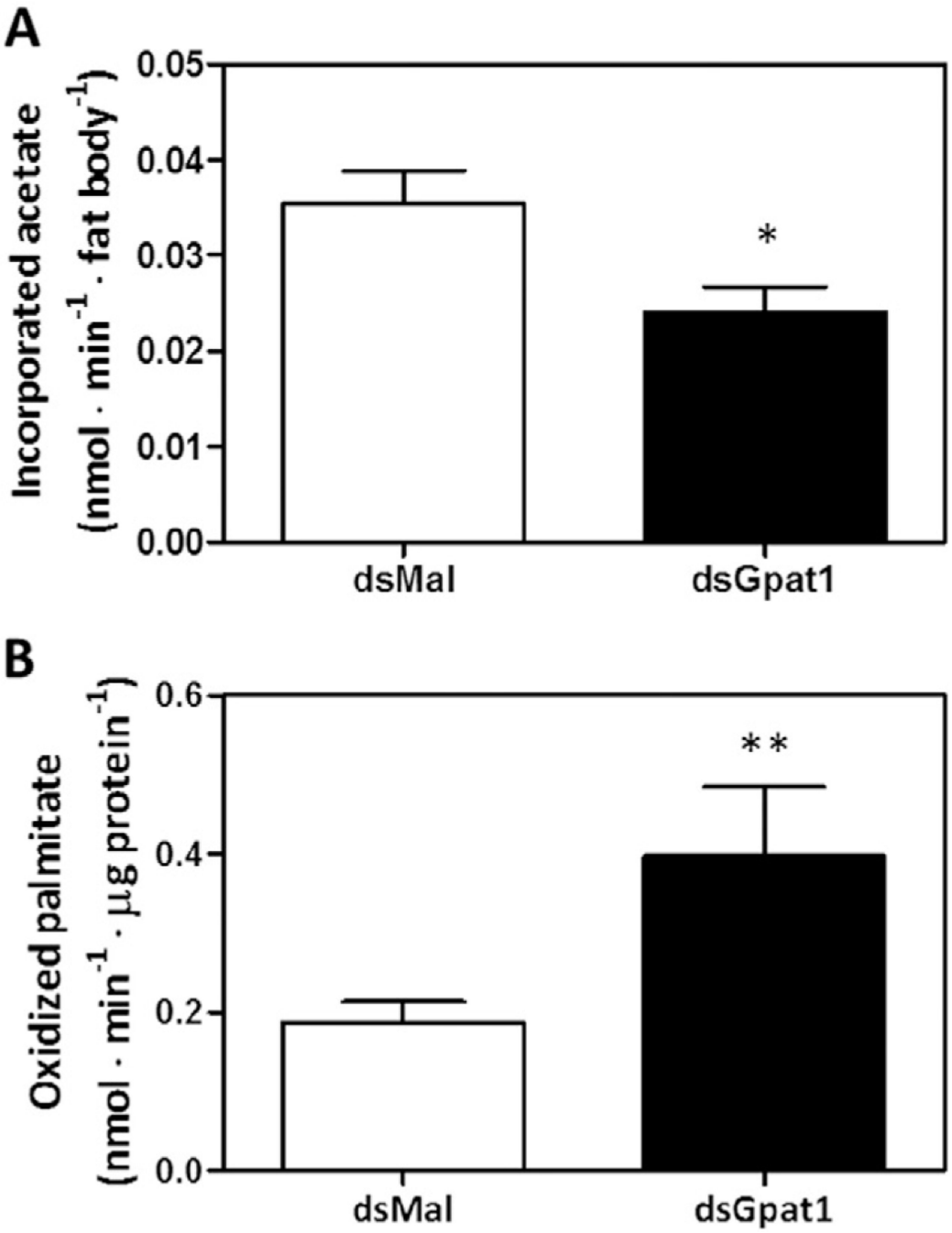

Fig. 9.

RhoprGpat1 knockdown decreases *de novo* synthesis of lipids and increases fatty acid oxidation in the fat body. Fasted adult females were injected with dsRNA for *RhoprGpat1* or *Mal* (control) genes. Insects were fed on the third day after injection. Fat bodies obtained at the 10th day after feeding were incubated with [^{3}H]-acetate to measure its incorporation into lipids (A). Alternatively, fat bodies were homogenized and incubated in the presence of

[^{3}H]-palmitate to measure lipid oxidation (B). Results are means ± S.E.M., n = 8–9 insects in 3 independent experiments. (*): $P < 0.05$ when compared to dsMal by Student's *t*-test.

Table 1

Acyltransferase motifs in GPATs.

Protein	Motif I	Motif II	Motif III	Motif IV
SacceSct1p	CAP**H**ANQFI**D**PA	GGIPVP**R**IQ **F**	P**EG**GSHDR	VAVV**P**CGLHY
SacceGpt2p	AAP**H**ANQFV**D**PV	MAIGVV**R**PQ **F**	P**EG**GSHDR	VKIV**P**CGMNY
RhoprGPAT1	LPL**H**R**S**HI**D**YIAV	LGAF**F**IK**R**RI	F**FIEG**GRTR	ALLV**P**VSVNYE
DromeGPAT1	VPL**H**R**S**HL**D**YIMV	LGAF**F**IK**R**KI F	**FIEG**GRTR	ALLV**P**VSVNYE
HomsaGPAT1	LPV**H**R**S**HI**D**YLLL	LGGF**F**IR**R**RL I	**FLEG**TRSR	ILII**P**VGISYD
MusmuGPAT1	LPV**H**R**S**HI**D**YLLL	LGGF**F**IR**R**RL I	**FLEG**TRSR	ILVI**P**VGISYD
HomsaGPAT2	LST**H**KTLL**D**GILL	LGGL**F**LPPEA I	**FLE**EPPGA	ALLV**P**VAVTYD
MusmuGPAT2	LST**H**K**S**LL**D**GFLL	LGGL**F**LPPEV I	**FLE**EPPGS	ATLV**P**VAIAYD
RhoprGPAT4	VAN**H**T**S**PI**D**ALIL	PQIW**F**ERSEV	I**F**P**EG**TCIN	GIIY**P**VAIKYD
DromeGPAT3	VAN**H**T**S**PI**D**VLVL	PHIW**F**ERGEA I	**FPEG**TCIN	GVIY**P**VAIKYD
DromeGPAT4	VAN**H**T**S**PI**D**VLVL	PHIW**F**ERGEA I	**FPEG**TCIN	GVIY**P**VAIKYD
HomsaGPAT3	VAN**H**T**S**PI**D**VLIL	PHVW**F**ERSEM I	**FPEG**TCIN	GTIH**P**VAIKYN
MusmuGPAT3	VAN**H**T**S**PI**D**VLIL	PHVW**F**ERSEI I	**FPEG**TCIN	GTIY**P**VAIKYN
HomsaGPAT4	VAN**H**T**S**PI**D**VIIL	PHVW**F**ERSEV I	**FPEG**TCIN	ATVY**P**VAIKYD
MusmuGPAT4	VAN**H**T**S**PI**D**VIIL	PHVW**F**ERSEV I	**FPEG**TCIN	ATVY**P**VAIKYD

GPAT sequences were aligned using the ClustalW algorithm. Grey boxes: highly conserved residues function (Based on Refs. [39–41]). Accession numbers of analyzed sequences are provided in Supplementary Table 2. Sacce, *Saccharomyces cerevisiae*; Rhopr, *Rhodnius prolixus*; Drome, *Drosophila melanogaster*; Homsa, *Homo sapiens*; Musmu, *Mus musculus*.